

An algorithm for the simulation of faulted bearings in non-stationary conditions

Gianluca D'Elia^a, Marco Cocconcelli^b, Emiliano Mucchi^a

^a*Department of Engineering, University of Ferrara, Via Saragat 1, 44122, Ferrara, Italy*

^b*Department of Sciences and Methods of Engineering, University of Modena and Reggio Emilia, Via Amendola 2 - Pad. Morselli, 42122, Reggio Emilia, Italy*

Abstract

In the field of condition monitoring the availability of a real test-bench is not so common. Furthermore, the early validation of a new diagnostic technique on a proper simulated signal is crucial and a fundamental step in order to provide a feedback to the researcher and to increase the chances of getting a positive result in the real case. In this context, the aim of this paper is to detail a step-by-step analytical model of faulted bearing that the reader could freely and immediately use to simulate different faults and different operating conditions. The vision of the project is a set of tools accepted by the community of researchers on condition monitoring, for the preliminary validation of new diagnostics techniques. The tool proposed in this paper is focused on ball bearing, and it is based on the well-known model published by Antoni in 2007. The features available are the following: selection of the location of the fault, stage of the fault, cyclostationarity of the signal, random contributions, deterministic contributions, effects of resonances in the machine and working conditions (stationary and non-stationary). The script is provided for the open-source Octave environment. The output signal is finally analysed to prove the expected features.

1

2 **1. Nomenclature**

$B(t)$	function which takes into account the purely cyclostationary content;
$COV\{\cdot\}$	covariance;
D	pitch circle diameter;
$E\{\cdot\}$	expectation operator;
F	amplitude of the force exciting the SDOF system;
L	vector length;
SNR	signal-to-noise ratio;
P_{noise}	noise power;
P_{signal}	signal power without noise;
T	inter-arrival time between two consecutive impacts;
d	bearing roller diameter;
f_c	carrier component of the rotation frequency;
f_d	frequency deviation of the rotation frequency;
f_m	frequency modulation of the rotation frequency;
$f_r(\theta)$	angular dependent rotation frequency;
f_s	sample frequency;
$h(t)$	impulse response to a single impact measured by the sensor;
k	SDOF system stiffness;
l	vector index;
m	SDOF system mass;

$p(t)$	function which takes into account periodic component;
$p_{rot}(\theta)$	deterministic part related to the rotation speed in the angular domain;
$p_{stiff}(\theta)$	deterministic part related to the stiffness variation in the angular domain;
$q(t)$	function which takes into account load distribution, bearing unbalance and periodic changes in the impulse response;
q_{rot}	positive number which weight the amplitude of $p_{rot}(\theta)$;
q_{stiff}	positive number which weights the amplitude of $p_{stiff}(\theta)$;
q_{Fault}	positive number governing the amplitude of the modulating function related to distributed fault;
$n(t)$	background noise;
n_r	number of rolling elements;
$x(t)$	simulated vibration signal;
$x_{SDOF}(t)$	time response of a SDOF system to unit impulse;
β	contact angle;
δ	Kronecker's symbol;
$\Delta\theta_{imp}$	angular position of a series of equispaced impulses;
ΔT_i	i th inter-arrival time;
$\Delta\theta_i$	i th angle between two consecutive impulses;
ε	error term;
ω_n	natural frequency of the SDOF system;
ω_d	damped natural frequency of the SDOF system;
σ^2	standard deviation;
τ_i	inter-arrival time jitters of the i th impact;

τ_{stiff}	geometrical bearing parameter related to the stiffness variation;
τ_{Fault}	geometrical bearing parameter related to the fault;
θ	angular variable;
ζ	damping coefficient of the SDOF system;

3 2. Introduction

4 Rolling bearings, together with gears, are one of the most studied com-
5 ponents. They are common components in mechanical design and they allow
6 the relative motion between two or more elements of the machine. Unfor-
7 tunately, the continuous movement between the parts of the bearing leads
8 to wear phenomena and subsequent failure. The degradation of the bearing
9 conditions can be revealed and monitored analysing the vibration signal pro-
10 duced by the contact among the bearing elements. There are other types of
11 techniques to determine the state of health of the bearings, such as moni-
12 toring the temperature or analysing the chemical content of the lubricant;
13 however, the vibration analysis is, de facto, the main technique used in con-
14 dition monitoring, despite the ease the noise and disturbances may enter into
15 the measurement. So far, thousand of algorithms have been published in the
16 literature trying to reject disturbances and to obtain a clear and telltale signal
17 to assess the health status of the bearing [1]. All these publications usually
18 provide results on both simulated signals and real measurements, more rarely
19 on only one of those. It is a matter of fact that the availability of a real test-
20 bench is not so common, and this is proven by the number of scientific papers
21 validated on few on-line available data centers (e.g. the Case Western Uni-
22 versity) providing real measurement data. On the contrary, simulated signals

23 are always available, since they are created on the same software for scientific
24 computing used in the post processing. The main advantage of a simulated
25 signal is to avoid the complexity of a real environment, focusing only on the
26 main contributions the developer decided to include. The main drawback is
27 that a too simple model may be too far from reality, making the proposed
28 algorithm not useful. The foundation of a faulted bearing simulation signal
29 is the model proposed by McFadden and Smith [2, 3, 4]. The bearing is
30 modelled as an epicyclic gear, where the inner ring is the sun gear, rolling
31 elements are the planet gears, the outer ring is the annular gear and the cage
32 is the planet carrier. This simple but powerful model allows the computation
33 of characteristics fault frequencies which are the fingerprints of a damage on
34 the bearing. Moreover, the model takes into account also the modulation ef-
35 fects due cyclic passage of the rolling elements on the load zone. Su and Lin
36 [5] studied the models under variable load due to shaft and roller errors. The
37 "gearbox" model for the bearings has a main limitation: the contact among
38 the bearing components is supposed to be a pure rolling contact, while some
39 slippery effect is always present due to the presence of the cage. Ho and Ran-
40 dall [8] proposed to model the bearing fault vibrations as a series of impulse
41 responses of a single-degree-of-freedom system, where the timing between the
42 impulses has a random component simulating the slippery effect. The next
43 fundamental contribution to the modelling of bearings came from the works
44 of Antoni and Randall [9, 11]. Starting from the work of Gardner [10], An-
45 toni and Randall proposed to model the vibration signal from a ball bearing
46 as a cyclostationary signal, i.e. a random process with a periodic autocorre-
47 lation function. Cyclostationarity better describes the effect of slippery and

48 has paved the way for later development. Most recent developments regard
49 the modelling of the vibration signal in non-stationary conditions [13], i.e.
50 taking into account the speed or load variations in the working conditions
51 of the machine. Unfortunately, as the proposed models have become more
52 detailed, the implementation of the algorithms has become more complex.
53 If the model of McFadden could be easily taught in an introductory course
54 at an engineering school, concepts like cyclostationarity and non-stationary
55 conditions are hardly present in advanced courses at engineering faculties.
56 As a consequence, it could be a gap between the theoretical description of a
57 vibration signal and the algorithm implemented to generate that vibration
58 signal on a computer. A wrong implementation leads to wrong simulated
59 signals used to test diagnostics procedures. In this scenario, the aim of this
60 paper is to provide a detailed step-by-step algorithm for the simulation of
61 the vibration signal provided by a faulted ball bearing. The script is devel-
62 oped in Octave environment, an open source high-level interpreted language,
63 primarily intended for numerical computations and quite similar to Matlab.
64 The base of this model is the one proposed by Antoni [6] with some im-
65 provements. In particular, the model of incipient faults at constant speed
66 has been extended to variable speed applications. In the distributed fault
67 model, the mathematical formulation is completely original and developed
68 by the authors of this paper. Details on the characteristics that the model
69 takes into account will be explained in the next sections. The final goal is
70 to start a discussion with the readers to define a bearing model that can be
71 used as a benchmark, recognized by the scientific community.

72 The paper is structured as follows: Section 3 covers the theoretical back-

73 ground of the bearing model and the numerical implementation. Section
74 4 focuses a numerical example, showing the output results of the proposed
75 algorithm. In Section 5 experimental end simulated data are compared to
76 validate the signal model. After the conclusions in Section 6, Appendix A
77 lists the script of the algorithm as Octave code.

78 3. Vibration signal model

79 3.1. Theoretical background

80 At first glance, the vibration signal model of a localized fault in a rolling
81 element bearing could be considered as the repetition of impact forces when
82 a defect in one bearing surface strikes a mating surface, which may excite
83 resonances in the bearing and in the machine. The repetition frequency of
84 these impacts uniquely depends on the defect location, being the defect on
85 the inner race, outer race, or in one of the rolling elements. Even if several
86 resonances can be present in the actual response, for simplicity, it will be
87 assumed in the remaining discussion that only one resonance occurs.

88 The vibration signal of a localized fault in a rolling element bearing can
89 be reasonably modelled as [6, 11]:

$$x(t) = \sum_{i=-\infty}^{+\infty} h(t - iT - \tau_i)q(iT) + n(t) \quad (1)$$

90 where $h(t)$ is the impulse response to a single impact as measured by the
91 sensor; $q(t)$ takes into account the periodic modulation due to the load dis-
92 tribution, possible bearing unbalance or misalignment, as well as the periodic
93 changes in the impulse response due to the movement of the faults towards
94 and backwards with respect to the sensor; T is the inter-arrival time between

95 two consecutive impacts; τ_i accounts for the uncertainties on the inter-arrival
 96 time (jitters) of the i th impact due to the necessary random slip of the rolling
 97 elements; $n(t)$ gathers the background noise.

98 Since this work focus the attention on the numerical implementation of
 99 Equation (1), instead of taking into account uncorrelated (white) jitters τ_i
 100 [6], an uncorrelated (white) inter-arrival time difference $\tau_{i+1} - \tau_i$ is used [11]:

$$E\{(\tau_{i+1} - \tau_i)(\tau_{j+1} - \tau_j)\} = \delta_{ij}\sigma_\tau^2 \quad (2)$$

101 where σ_τ is the standard deviation and δ_{ij} is the Kronecker's symbol. Even if
 102 Equation (1) embodies a well defined harmonic structure, the presence of very
 103 slight random fluctuations of the inter-arrival time of consecutive impulses
 104 causes the rapidly turns of the signal into a random one. Therefore, weak
 105 harmonic components can be located in the lower-frequency range, and a
 106 dominating random cyclostationary component can be located in the higher-
 107 frequency range (pseudo-cyclostationary). A detailed theoretical explanation
 108 of the frequency content of Equation (1) can be found in [6, 11].

109 When a localized fault propagates on the surface where it was initiated, a
 110 larger area of the bearing becomes involved in the genesis of the vibration sig-
 111 nature. In this scenario, no sharp impulses are generated, but the fault signa-
 112 ture becomes purely cyclostationary (as opposed to pseudo-cyclostationary)
 113 [14, 9]. This pure cyclostationary content is the result of a randomly dis-
 114 tributed phase, caused by the different position on the rough surface of the
 115 rolling elements for every revolution. However, strong periodic components
 116 are generated at the shaft periodicity, when the fault only extends over a
 117 limited sector of the race. Moreover, if the bearing is highly loaded, a pe-
 118 riodic component can be initiated by the bearing stiffness variation due to

119 the changing numbers and positions of the rolling elements in the load zone.
 120 The distributed fault vibration signature may be written [9]:

$$x_d(t) = p(t) + B(t) \quad (3)$$

121 where $p(t)$ accounts for the periodic component such as shaft and stiffness
 122 variation periodicities and $B(t)$ for the purely cyclostationary content with
 123 $E\{B(t)\} = 0$.

124 3.2. Numerical implementation

125 This work focuses the attention on the numerical implementation of the
 126 vibration signal models of Equations (1) and (3). In particular, these models
 127 are extended to cover generic speed profile of the bearing shaft. In order to
 128 include a speed variation, the vibration signal is firstly defined in the angle
 129 domain and then transformed back to the time domain according with the
 130 chosen speed profile.

131 Let $\theta(t)$ be the rotation angle of a bearing moving race (inner and/or
 132 outer). Without loss of generality, in the following the bearing outer race is
 133 considered fixed whilst the inner race is rotating. A generic speed profile in
 134 the angle domain can be constructed as:

$$f_r(\theta) = f_c + 2\pi f_d \int \cos(f_m \theta) d\theta \quad (4)$$

135 where f_c is the carrier component of the rotation frequency, f_d is the fre-
 136 quency deviation and f_m is the frequency modulation. The main terms (f_c ,
 137 f_d and f_m) of Equation (4) can or cannot be angle dependent. Figure 1
 138 depicts an example of Equation (4) for a case of sinusoidally speed varying
 139 profile. Without loss of generality, hereafter it is assumed that at time $t = 0$

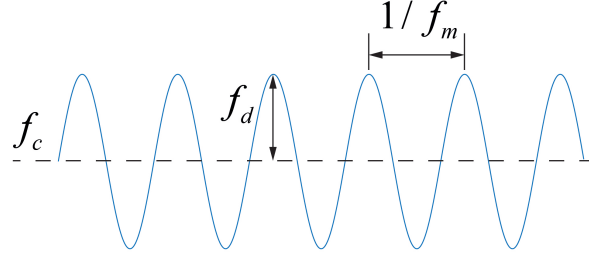


Figure 1: Example of sinusoidally speed varying profile.

140 the defect is located at the position $\theta = 0$ and it is in contact with a rolling
 141 element.

142 Concerning localized fault in ball bearing, the angle between two consec-
 143 utive impulses can be easily obtained from the "gearbox" model of the rolling
 144 element bearing (see Table 1 for the usual bearing fault frequencies), for a
 145 inner-race fault:

$$\Delta\theta_{imp} = \frac{2\pi}{\frac{n_r}{2}(1 + \frac{d}{D}\cos\beta)} \quad (5)$$

146 Equation (5) can be used to obtain the angular position of a series of
 147 equispaced impulses, i.e. a purely deterministic signal. As stated before, in
 148 order to take into account the necessary random slip of the rolling elements a
 149 random contribution must be added to Equation (5). The angle between two
 150 consecutive impulses is strictly positive, and so the gamma law is the best
 151 candidate; nonetheless when the variance is low with respect to the mean
 152 value, the gamma distribution is well approximated by a normal distribution
 153 with the same mean and variance. In this work, the random contribution
 154 is taken into account by generating normally distributed random numbers
 155 with mean $\Delta\theta_{imp}$ and variance $\sigma_{\Delta\theta}^2$. As the speed profile is defined in terms

156 of rotation angle θ (Equation (4)), the inter-arrival time among the impulses
 157 can be obtained by the generated random numbers as:

$$\Delta T_i = \frac{\Delta \theta_i}{2\pi f_r(\theta)} \quad (6)$$

158 where ΔT_i is the i th inter-arrival time, $\Delta \theta_i$ is the i th angle between two
 159 consecutive impulses randomly generated with mean $\Delta \theta_{imp}$ and variance $\sigma_{\Delta \theta}^2$
 160 and $f_r(\theta)$ is the angular dependent rotation frequency.

161 The results of Equation (6) are the inter-arrival times of each impulse with
 162 the speed profile defined in Equation (4). These times define the beginning
 163 of each impulse response $h(t - iT - \tau_i)$ in the time signal itself; such a signal
 164 can be obtained in a Matlab/Octave environment as follows:

- 165 1. generate a L point vector filled with zeros, corresponding at times $t =$
 166 l/f_s , where f_s is the sample frequency in Hz and l is a index ranging
 167 from 0 to $L - 1$,
- 168 2. place 1 at index values obtained by dividing each inter-arrival time ΔT_i
 169 by the chosen sample frequency f_s ,
- 170 3. weight the so generated vector with the weighting function $q(iT)$,
- 171 4. filter the weighted vector with the FFT-based method of overlap-add by
 172 choosing as filter coefficients the impulse response function of a SDOF
 173 system in terms of acceleration.

174 Several methods can be found in the literature in order to obtain the im-
 175 pulse response of a SDOF system [8, 15]; they deal with the implementation
 176 of such a response in the frequency domain and then transform it back in
 177 the time domain via the Inverse Fourier Transform. However, this procedure
 178 involves the generation of a low pass filter as well as a phase correction [8]. In

179 this work the authors decided to generate the response of the SDOF system
 180 to unit impulse in the time domain as:

$$x_{SDOF}(t) = \frac{F/m}{\omega_d} e^{-\zeta\omega_n t} \sin(\omega_d t) \quad (7)$$

181 where F is the amplitude of the force exciting the SDOF system, m the
 182 system mass, ζ the damping coefficient, ω_n the natural frequency in [rad/s]
 183 and $\omega_d = \omega_n \sqrt{1 - \zeta^2}$. The response in terms of acceleration can be simply
 184 obtained by a double derivative with respect to time. In this scenario, the
 185 numerical derivative does not add high frequency noise inside the signal,
 186 because no noise is present in the generated $x_{SDOF}(t)$.

187 From the procedure heretofore described, the key point is to find inside
 188 the time signal, the index l corresponding to the beginning of the impulse. De
 189 facto, l must be an integer number. However by dividing ΔT_i by the selected
 190 sample frequency f_s , a rational number is usually obtained. Instead of using
 191 an interpolation procedure on the time signal itself, the authors decide to
 192 rounding the rational numbers to the nearest integers. With this operation,
 193 an error is introduced that depends on the selected sample frequency f_s (the
 194 greater f_s , the lower is the error), which affects both mean and variance of
 195 the theoretical ΔT_i . Let $\overline{\Delta T_i}$ the value of ΔT_i obtained via the rounding
 196 procedure, the error term is:

$$\varepsilon = \overline{\Delta T_i} - \Delta T_i \quad (8)$$

197 with mean and variance:

$$E\{\varepsilon\} = E\{\overline{\Delta T_i}\} - E\{\Delta T_i\} \quad (9)$$

$$\sigma_\varepsilon^2 = \sigma_{\overline{\Delta T_i}}^2 + \sigma_{\Delta T_i}^2 - 2COV\{\overline{\Delta T_i}, \Delta T_i\}$$

198 Finally, the last term of Equation (1) which deals with the noise compo-
 199 nent, can be added to the signal by generating randomly distributed number
 200 with a given power. The power of the noise can be set with a desired Signal-
 201 to-Noise Ratio (SNR), which is a measure that compares the level of a desired
 202 signal to the level of background noise. The SNR is defined as:

$$SNR = 10 \log_{10} \left(\frac{P_{signal}}{P_{noise}} \right) \quad (10)$$

203 where P_{signal} is the power of the signal without noise and P_{noise} is the noise
 204 power. Figure 2 depicts the schema of the proposed procedure. Moreover,
 205 in Appendix A an Octave function called *bearingSignalModelLocal* has been
 206 inserted in order to easily implement Equation (1).

207 The same procedure can be efficiently extended for the case of distributed
 208 faults in rolling element bearing. This vibration signal model is a mixture of
 209 two terms, one deterministic and one purely cyclostationary. Once the speed
 210 profile has been defined with respect to rotation angle θ , the deterministic
 211 part can be described in the angular domain as:

$$p_{rot}(\theta) = q_{rot} \cos \left(\frac{f_c}{f_c} \theta + \frac{f_d}{f_c} \int \cos \left(\frac{f_m}{f_c} \theta \right) d\theta \right) \quad (11)$$

$$p_{stiff}(\theta) = q_{stiff} \cos \left(\frac{f_c}{f_c} \tau_{stiff} \theta + \frac{f_d}{f_c} \tau_{stiff} \int \cos \left(\frac{f_m}{f_c} \tau_{stiff} \theta \right) d\theta \right)$$

212 where q_{rot} and q_{stiff} are two positive numbers which weigh the amplitude of
 213 the deterministic components, whilst τ_{stiff} is a geometrical bearing parameter
 214 which can be obtained by the "gearbox" bearing model as:

$$\tau_{stiff} = \frac{n_r}{2} \left(1 - \frac{d}{D} \cos \beta \right) \quad (12)$$

215 De facto, in rolling element bearings, the frequency of the stiffness variation
 216 is equal to the frequency of an outer-race fault. As done before, by the

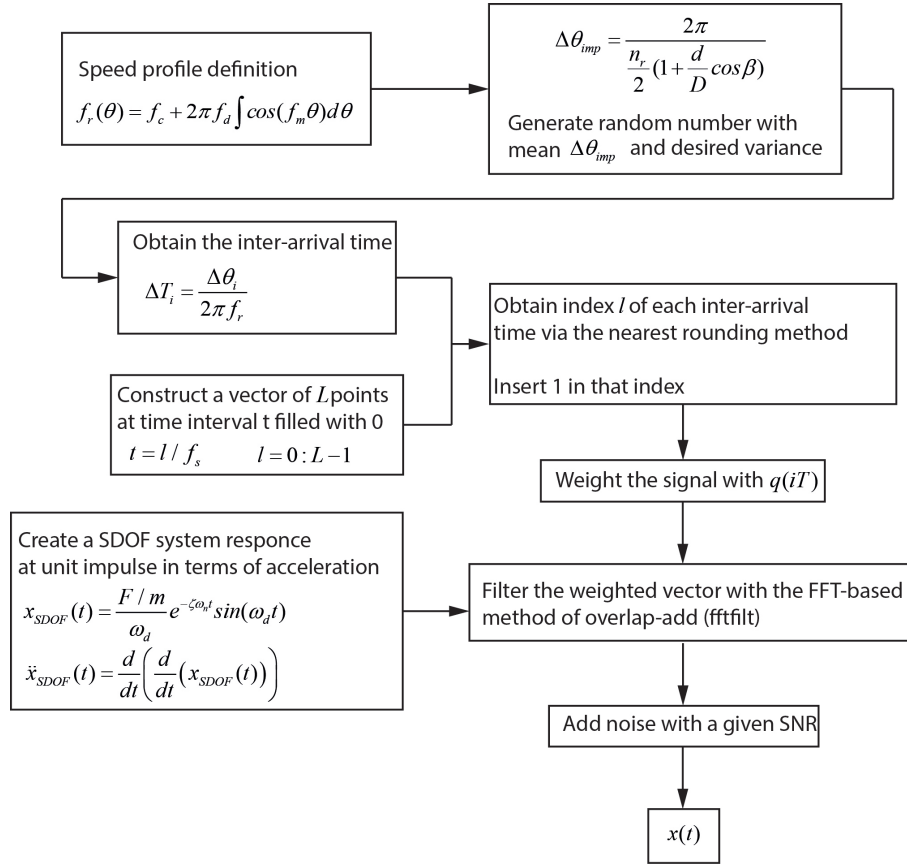


Figure 2: Schema for the numerical implementation of Equation (1).

217 knowledge of the speed profile, the angle signals can be transformed by a
218 simple interpolation in the time domain.

219 The purely cyclostationary component ($B(t)$) is a random modulated
220 noise, where the modulation frequency is the fault frequency. Once the speed
221 profile is selected, the modulating function for an inner-race fault (see Table
222 1 for other types of fault), can be expressed in the angle domain as:

$$q(\theta) = 1 + q_{Fault} \sin\left(\frac{f_c}{f_c} \tau_{Fault} \theta + \frac{f_d}{f_c n_r} \tau_{Fault} \int \cos\left(\frac{f_m}{f_c n_r} \tau_{Fault} \theta\right) d\theta\right) \quad (13)$$

223 where q_{Fault} is a number governing the amplitude of the modulating function
 224 and τ_{Fault} is a geometrical parameter which can be obtained by the "gearbox"
 225 model of the rolling element bearing as:

$$\tau_{Fault} = \frac{n_r}{2} \left(1 + \frac{d}{D} \cos \beta\right) \quad (14)$$

226 Equation (13) can be transformed in the time domain by a simple interpo-
 227 lation and the purely cyclostationary component can be obtained by modu-
 228 lating normally distributed random number with the time domain $q_{Fault}(t)$.
 229 Finally, stationary noise can be added to the signal with a given SNR via the
 use of Equation (10). Figure 3 depicts the schema of the proposed procedure.

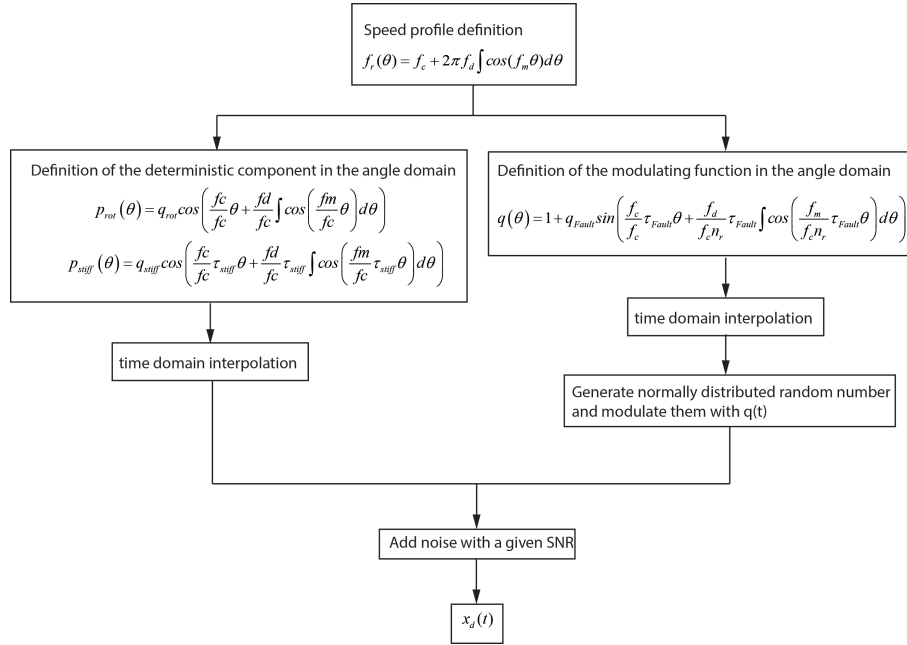


Figure 3: Schema for the numerical implementation of Equation (3).

230

231 Moreover, in Appendix A an Octave function called *bearingSignalModelDist*
 232 has been inserted in order to easily implement Equation (3).

233 **4. Numerical Example**

234 Table 1 depicts the typical equation for the evaluation of bearing fault
 235 frequencies as well as the bearing dimensions used in the numerical examples,
 236 whilst Table 2 shows the vibration signal model parameters.

Fault frequencies [Hz]		Geometrical parameters	
Inner-race fault	$\frac{n_r}{2} f_r (1 + \frac{d}{D} \cos \beta)$	Bearing roller diameter (d) [mm]	21.4
Outer-race fault	$\frac{n_r}{2} f_r (1 - \frac{d}{D} \cos \beta)$	Pitch circle diameter (D) [mm]	203
Rolling-element fault	$\frac{f_r d}{D} (1 - (\frac{d}{D} \cos \beta)^2)$	Number of rolling elements (n_r)	23
Cage fault	$\frac{f_r}{2} (1 - \frac{d}{D} \cos \beta)$	Contact angle (β) [deg]	9.0

Table 1: **Typical fault frequencies and bearing dimensions**

237 As stated beforehand, a speed profile has to be generated. The selected
 238 speed profile used hereafter in the numerical examples is depicted in Figure
 239 4, and it deals with a constant rotation frequency of 10Hz modulated at 1Hz
 240 with an amplitude of 0.8Hz (see Table 2). From now on both localized and
 241 distributed faults in the inner-race of a rolling element bearing are taken into
 242 account (see Appendix A for Octave scripts). The mean and variance of the
 243 random contribution related to the rolling element slips are set in the angle
 244 domain as $\Delta\theta_{imp}$ and $0.04\Delta\theta_{imp}$ respectively, that lead to $7.8981E - 3$ (the
 245 inverse of the fault frequency) and $3.0224E - 07$ due to the selected speed
 246 profile. As stated in the previous section, the impulse locations in the time
 247 domain signal are approximated by a neighbour interpolation that introduces
 248 an error term in both the selected mean and variance, which is related to the
 249 sample frequency of the time signal itself. In particular, the final mean and
 250 variance are $7.8980E - 3$ and $3.0245E - 07$ showing that the error is negligible

Vibration Signal Model Parameters	Localized fault Ex.	Distributed fault Ex.
Number of shaft revolutions	1E4	1E4
Number of points per revolution	2048	2048
Sample frequency f_s [Hz]	20E3	20E3
Carrier component of the shaft speed f_c [Hz]	10	10
Frequency deviation f_d [Hz]	$0.08f_c$	$0.08f_c$
Modulation frequency f_m [Hz]	$0.1f_c$	$0.1f_c$
SDOF spring stiffness k [N/m]	2E13	/
SDOF damping coefficient ζ	5%	/
SDOF natural frequency f_n [Hz]	6E3	/
Amplitude modulation for localized fault	0.3	/
Amplitude value of the deterministic component related to the stiffness variation q_{stiff}	/	0.1
Amplitude value of the deterministic component related to the bearing rotation q_{rot}	/	0.1
Amplitude value of the amplitude modulation at the fault frequency q_{Fault}	/	1
Signal to Noise Ratio [dB]	0	0
Expected fault frequencies		
Inner-race fault frequency [Hz]	≈ 126.97	≈ 126.97
Inner-race fault order [O]	12.69	12.69

Table 2: Vibration signal model data for localized and distributed faults in rolling elements bearing.

251 in the generation of the vibration signal for the usual sample frequencies.

252 Figure 5 depicts the simulated time signal in case of inner-race local-
253 ized fault following the data of Table 2. At a first glance, the signal seems
254 strictly deterministic, showing a series of impulse responses (Figure 5(a,b)).
255 However, the random slips of the rolling elements turn the signal to strictly
256 random. This effect can be easily seen from the PSD signal. Figure 5(c)
257 plots the PSD computed with the Welch's method, by using an Hanning
258 window with a 75% of overlap. It is clearly visible from the PSD signal that
259 the noise signal is purely random in nature, in particular the harmonic series

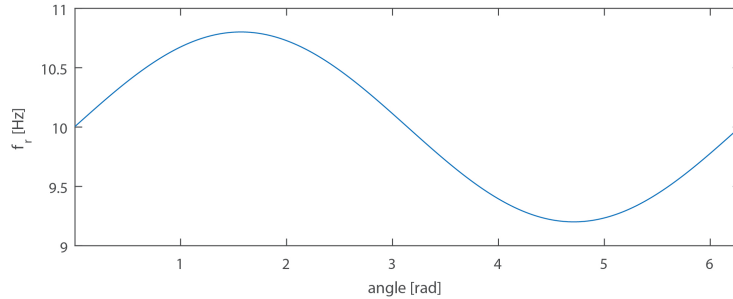


Figure 4: Speed profile used in the numerical examples for a complete revolution of the inner race.

260 related to the repetition of the impulses are strongly masked by the back-
 261 ground noise and die quickly. De facto, Antoni and Randall [6, 11] proved
 262 that the decay of the harmonic structure strictly depends on the selected
 263 variance due to the low-pass filter nature of Equation 1. In order to high-
 264 light the fault frequency cyclostationary analysis has to be carried out. The
 265 main signal processing technique in the cyclostationary field is Spectral Cor-
 266 relation Density function (SCD), which depicts the cyclostationary content
 267 with respect to the frequency content of the signal. This technique has to
 268 be used in case of constant speed, however when the speed is changing a
 269 cyclo-non-stationary signal is generated. G. D'Elia et al. [14] were the firsts
 270 to explore the order-frequency approach extending the SCD to speed varying
 271 signals. D. Abboud et al. [17] proposed a more rigorous approach to the anal-
 272 ysis of cyclo-non-stationary signals. Figure 7(a) depicts the Order-Frequency
 273 Spectral Correlation function (OFSC) for the synthesized signal in case of
 274 localized fault. It is possible to see how the order related to the inner-race
 275 fault (see Table 2) is highlighted around a frequency region of 6kHz, which

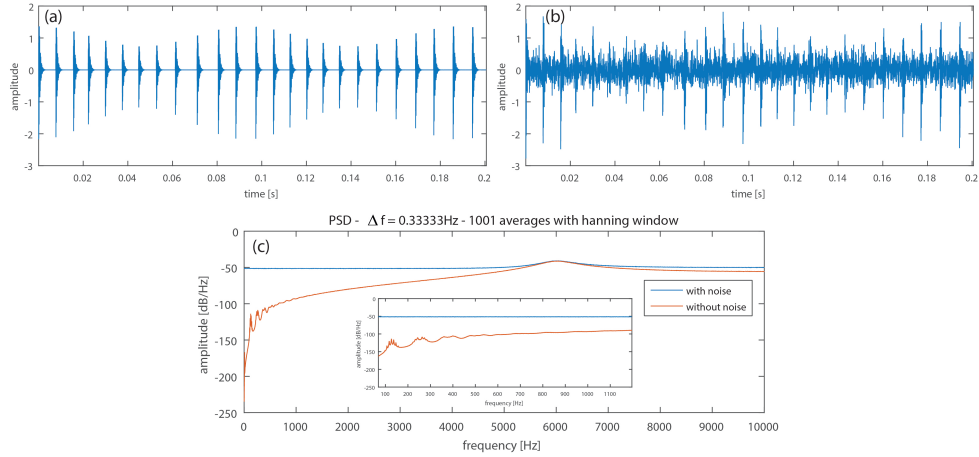


Figure 5: Simulated vibration signal in case of inner-race localized fault: (a) without noise, (b) with noise, (c) Power Spectral Density (PSD).

276 is the resonance frequency excited by the bearing impulses. Moreover, the
 277 OFSC also highlights the amplitude modulation due to the periodic variation
 278 of the load distribution.

279 Figures 6(a,b) depict the time signal for a inner-race distributed fault with
 280 and without noise addiction. It is possible to see how the signal seems strictly
 281 random. In particular, even without noise the deterministic component re-
 282 lated to the stiffness variation as well as shaft rotation are hidden. Figure
 283 6(c) highlights the PSD of such a signal, where the random contribution is
 284 clearly visible in the medium/high frequency range, whilst the determinis-
 285 tic components are depicted in the low frequency region. Moreover, due to
 286 the speed variation, modulation around the bearing stiffness variation fre-
 287 quency can be easily detected. As done before, in order to highlight the fault
 288 frequency the OFSC function is evaluated on the simulated signal. Figure

289 7(b) plots the result of these operations. The cyclic order frequency con-
 290 cerning the inner-race fault (12.650) is clearly visible in the entire frequency
 291 range, focusing the broad band phenomenon involved in the distributed fault
 signature.

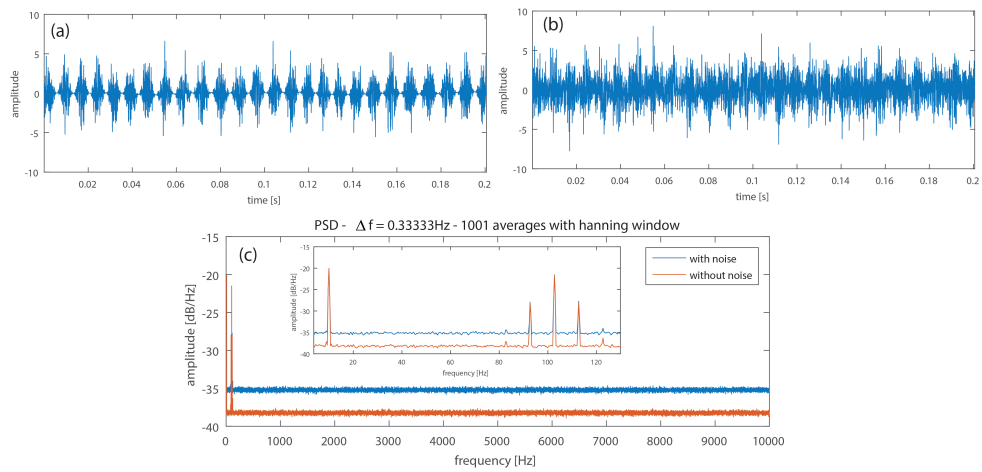


Figure 6: Simulated vibration signal in case of inner-race distributed fault: (a) without noise, (b) with noise, (c) Power Spectral Density (PSD).

292

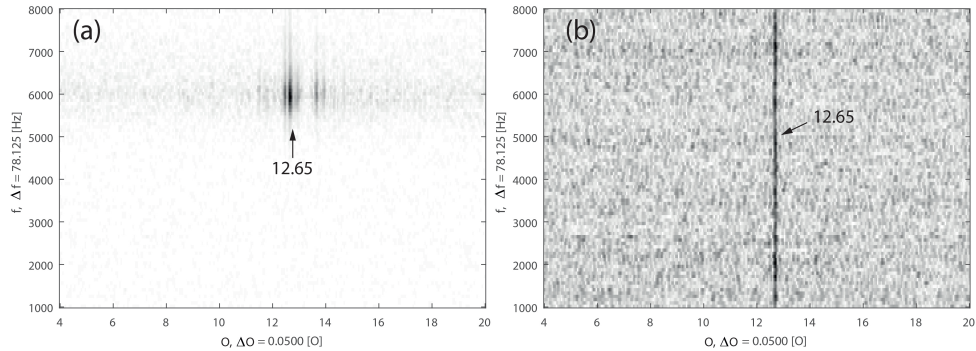


Figure 7: Order-Frequency Spectral Correlation Function (OFSC): (a) localized fault, (b) distributed fault.

293 5. Experimental validation

294 In this section, the proposed algorithm is validated on experimental data
 295 of faulted bearing. The data are provided by Prof. Gareth Forbes at Cur-
 296 tain University, by Creative Commons Attribution 4.0 International License,
 297 through the Data-acoustics.com Database [18]. The provided Matlab files
 298 contain radial vibration measurements on the bearing housing of the Spectra-
 299 traQuest Machinery Fault Simulator test rig. The set of measurements con-
 300 tain two files: a known inner and outer race bearing fault, respectively. The
 301 validation of the algorithm focuses on the outer race bearing fault case. The
 302 measured parameters are:

- 303 • Radial Bearing Housing Acceleration (m/s^2)
- 304 • Tacho - once per revolution pulse (Volts)

305 Bearing dimensions and setup characteristics are listed in Table 3. Figure 8
 306 shows the raw data loaded from file and the corresponding spectrum.

Bearing and setup information

Bearing No.	MB ER-16K	Sampling frequency	51200 [Hz]
Number of balls	9	Length of record	10 [s]
Ball Diameter	7.9375 [mm]	Rotational speed	29 [Hz]
Pitch Diameter	38.50 [mm]	BPFO	103.588 [Hz]

Table 3: Bearing and setup information of the experimental test on a outer race fault.

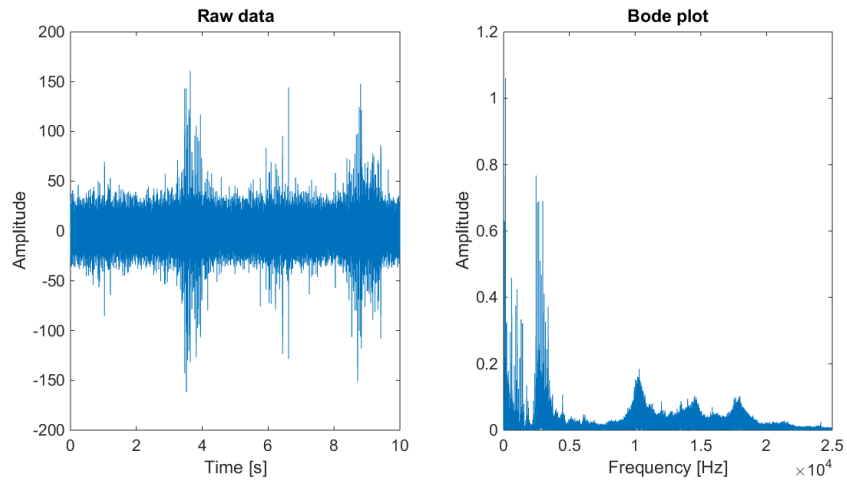


Figure 8: Raw data in time and frequency domains.

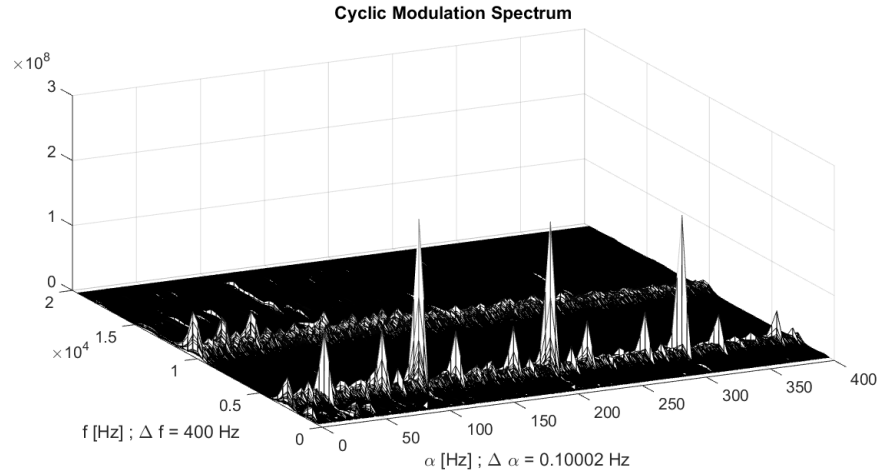


Figure 9: Cyclic modulation spectrum of raw data.

307 First, the raw data is analyzed to characterize the frequency content.
 308 Since the bearing data is a cyclostationary signal [6], the cyclic modulation
 309 spectrum of the raw data is shown in Figure 9.

310 The spectrum is characterized by three main components at Ball Pass
 311 Frequency of Outer ring (BPFO) and harmonics (α -axis). Moreover, there is
 312 a relevant component at rotational frequency of the shaft (29 Hz) and suc-
 313 cessive harmonics. Probably there is an imbalance on the shaft, although not
 314 reported on the test description. The signal has a resonance band around
 315 2800 Hz (f -axis) and a secondary one around 10400 Hz. It must be noted
 316 that the fault components are present at the first resonance only, while the
 317 imbalance of the shaft is present on both resonances. The simulation of
 318 the faulted bearing will focus on the outer race fault components only, not
 319 covering the imbalance effects. From the tachometer signal the instantaneous ro-
 320 tational speed in angle is computed (Figure 10), verifying that the test was

321 done at constant speed with a small fluctuation of the rotational speed. The
322 speed profile is given as input to the signal model, providing also the bear-
323 ing information of Table 3 and resonance frequency highlighted in the cyclic
324 modulation spectrum (Figure 9). In addition to the parameters listed in Ta-
325 ble 3, the used model variables are collected in Table 4. It is worth noting
326 that the carrier component of the shaft speed (f_c), the frequency deviation
327 (f_d) and the modulation frequency (f_m) are not necessary, since the instan-
328 taneous rotational frequency is directly computed from the tacho signal. The
329 output data are compared with experimental raw data in Figure 11. The time
330 domain comparison highlights that the signal periodicity is captured by the
331 simulated signal, albeit differences in terms of signal amplitude occurs. How-
332 ever, it has to be underlined that the primary goal of a signal model is to
333 correctly represent the frequency content of the experimental signal, less its
334 amplitude. Finally, Figure 12 shows the cyclic modulation spectrum of the
335 faulted bearing simulated signal. The characteristic fault frequency and its
336 harmonics are evident, like in the experimental cyclic modulation spectrum
337 in Figure 9. The spectrum components at the rotational frequency and har-
338 monics are not present since the model focuses on the fault component only,
339 but may be added. Moreover, the simulated signal exhibits the resonance
340 frequency at 2800 Hz as given in Table 4.

Vibration Signal Model Parameters

Number of shaft revolutions	284
Number of points per revolution	2048
Sample frequency f_s [Hz]	51200
SDOF spring stiffness k [N/m]	$2E13$
SDOF damping coefficient ζ	4%
SDOF natural frequency f_n [Hz]	2800
Amplitude modulation for localized fault	1
Signal to Noise Ratio [dB]	3

Table 4: **Vibration signal model data use for experimental validation.**

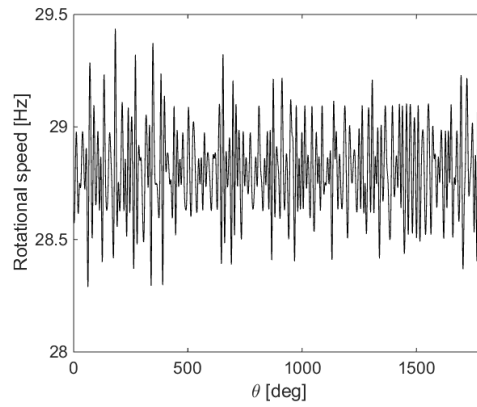


Figure 10: **Instantaneous angular speed.**

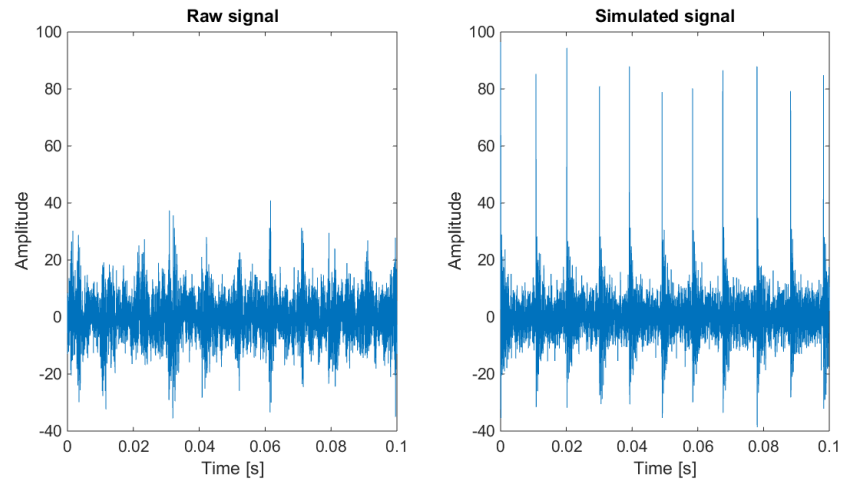


Figure 11: Comparison between experimental and simulated vibration signals.

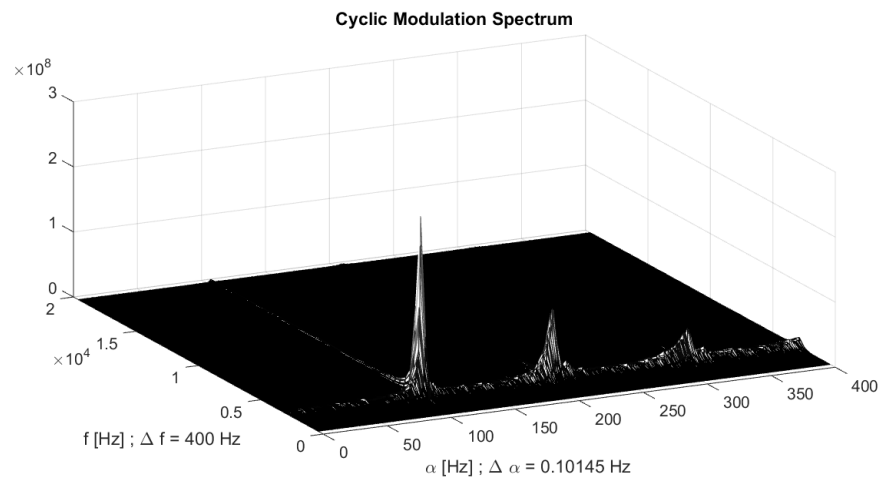


Figure 12: Cyclic modulation spectrum of simulated data.

341 **6. Conclusion**

342 This paper details an algorithm to simulate the expected vibration signal
343 of a faulted bearing. The model is based on the work of Antoni [6], with some
344 improvements. In particular, the model of incipient faults at constant speed
345 has been extended to variable speed applications. In the distributed fault
346 model, the mathematical formulation is completely original and developed
347 by the authors of this paper. The basic features that the user could set are:

- 348 • selection of the location of the fault (e.g. outer ring, inner ring, etc...),
- 349 • selection of the stage of the fault (e.g. punctual fault, distributed fault,
350 etc...),
- 351 • cyclostationarity of the signal,
- 352 • random contributions,
- 353 • deterministic contributions,
- 354 • effects of resonances in the machine,
- 355 • working conditions (stationary and non-stationary).

356 This project has been developed under a Creative Commons license and
357 the vision of the project is a set of tools accepted by the community of re-
358 searchers on condition monitoring, for the preliminary validation of new di-
359 agnostics techniques. The reader could freely and immediately use the script
360 in Appendix A to simulate different faults and different operating conditions.
361 The script is provided for the open-source Octave environment. The paper

362 fully details the theoretical background and the numeric implementation of
363 the vibration model. Examples of the output signals for simulated faulty
364 bearings (localized and generalized faults) have been shown and commented.
365 Finally, the model is validated on experimental data of a faulted bearing,
366 provided by data-acoustics.com database under the Creative Common Attri-
367 bution license. The simulated signal has the same resonance frequency and
368 fault-related components of the experimental data.

369 This work is licensed under the Creative Commons Attribution-ShareAlike
370 4.0 International License.

371 To view a copy of the license, visit [http://creativecommons.org/licenses/by-](http://creativecommons.org/licenses/by-sa/4.0/)
372 [sa/4.0/](http://creativecommons.org/licenses/by-sa/4.0/)



373 **Acknowledgment**

374 Acknowledgement is made for the measurements used in this work pro-
375 vided through data-acoustics.com Database. In particular, the authors thank
376 Prof. Gareth Forbes at Department of Mechanical Engineering of Curtin Uni-
377 versity (Australia), who provided the experimental data through Creative
378 Commons Attribution 4.0 International License.

379 **Compliance with Ethical Standards**

380 The authors declare that they have no conflict of interest.

381 **7. References**

- 382 [1] I. El-Thalji, E. Jantunen, *A summary of fault modelling and predictive*
383 *health monitoring of rolling element bearings*, Mechanical Systems and
384 Signal Processing, Vol. 60 (2015), pp. 252-272.
- 385 [2] P.D. McFadden, J.D. Smith, *Vibration monitoring of rolling element*
386 *bearings by the high frequency resonance technique a review*, Tribology
387 International, Vol. 117 (1984), pp. 3-10.
- 388 [3] P.D. McFadden, J.D. Smith, *Model for the vibration produced by a single*
389 *point defect*, Journal of Sound and Vibration, Vol. 96 (1984), pp. 69-82.
- 390 [4] P.D. McFadden, J.D. Smith, *The vibration produced by multiple point*
391 *defects in a rolling element bearing*, Journal of Sound and Vibration,
392 Vol. 98 (1984), pp. 263-273.
- 393 [5] Y.T. Su, S.J. Lin, *On initial detection of a tapered roller bearing fre-*
394 *quency domain analysis*, Journal of Sound and Vibration, Vol. 155
395 (1992), pp. 75-84.
- 396 [6] J. Antoni, *Cyclic spectral analysis of rolling-element bearing signals:*
397 *Facts and fictions*, Journal of Sound and Vibration, Vol. 304 (2007),
398 pp. 497-529.
- 399 [7] J.I. Taylor, *Identification of Bearing Defects by Spectral Analysis*, Jour-
400 *nal of Mechanical Design*, Vol. 102 (1980), pp. 199-204.
- 401 [8] D. Ho, R.B. Randall *Optimisation of bearing diagnostic techniques us-*

- 402 *ing simulated and actual bearing fault signals*, Mechanical Systems and
403 Signal Processing, Vol. 14 (2000), pp. 763-788.
- 404 [9] J. Antoni, R.B. Randall *Differential Diagnosis of Gear and Bearing*
405 *Faults*, Journal of Vibration and Acoustics, Vol. 124 (2002), pp. 165-
406 171.
- 407 [10] W.A. Gardner, *Introduction to random processes with application to sig-*
408 *nals and systems*, Macmillan, New York.
- 409 [11] J. Antoni, R.B. Randall, *A Stochastic Model for Simulation and Diag-*
410 *nostics of Rolling Element Bearings With Localized Faults*, Journal of
411 Vibration and Acoustics, Vol. 125 (2003), pp 282-289.
- 412 [12] R.B. Randall, J. Antoni, S. Chobsaard, *The relationship between spectral*
413 *correlation and envelope analysis in the diagnostics of bearing faults and*
414 *other cyclostationary machine signals*, Mechanical Systems and Signal
415 Processing, Vol. 15 (2001), pp. 945-962
- 416 [13] A. Bourdon, H. André, D. Rémond, *Introducing angularly periodic dis-*
417 *turbances in dynamic models of rotating systems under non-stationary*
418 *conditions*, Mechanical Systems and Signal Processing, Vol. 44 (2014),
419 pp. 60-71
- 420 [14] G. D'Elia, S. Delvecchio, M. Cocconcelli, E. Mucchi, G. Dalpiaz, *Ap-*
421 *plication of cyclostationary indicators for the diagnostics of distributed*
422 *faults in ball bearings*, Proceedings of the ASME 2013 International De-
423 sign Engineering Technical Conferences & Computers and Information

424 in Engineering Conference IDETC/CIE 2013. August 4-7, 2013, Port-
425 land.

426 [15] J.B. Roberts, *On the reponse of a simple oscillator to random impulses*,
427 Journal of Sound and Vibration, Vol. 4 (1966), pp. 51-61.

428 [16] G. D'Elia, Z. Daher, J. Antoni, *A novel approach for the cyclo-non-*
429 *stationary analysis of speed varying signals*, Proceedings of ISMA 2010.
430 September 22-27, 2010, Leuven Belgium.

431 [17] D. Abbod, S. Baudin, J. Antoni, D. Rémond, M. Eltabach, O. Sauvage,
432 *The spectral analysis of cyclo-non-stationary signals*, Mechanical Sys-
433 tems and Signal Processing, Vol. 75 (2016), pp. 280-300.

434 [18] Data-acoustics.com, *Inner and Outer Race Bearing Fault Vibration*
435 *Measurements*, <http://data-acoustics.com/?p=202>

436 Appendix A. Octave Code

```
437 %% Simulated localized and distributed fault in rolling
438 % element bearing
439 %
440 % G. D'Elia and M. Cocconcelli
441
442 clear
443 clc
444
445 %% Bearing geometry
446 d = 21.4; % bearing roller diameter [mm]
447 D = 203; % pitch circle diameter [mm]
448 n = 23; % number of rolling elements
449 contactAngle = 9*pi/180; % contact angle
```

```

450 faultType = 'inner';
451
452 %% Speed profile
453 N = 2048; % number of points per revolution
454 Ltheta = 10000*N; % signal length
455 theta = (0:Ltheta-1)*2*pi/N;
456 fc = 10;
457 fd = 0.08*fc;
458 fm = 0.1*fc;
459 fr = fc + 2*pi*fd.*(cumsum(cos(fm.*theta)/N));
460
461 %% Localized fault
462 varianceFactor = 0.04;
463 fs = 20000; % sample frequency [Hz]
464 k = 2e13;
465 zita = 5/100;
466 fn = 6e3; % natural frequency [Hz]
467 Lsdof = 2^8;
468 SNR_dB = 0;
469 qAmpMod = 0.3;
470 [tLocal, xLocal, xNoiseLocal, frTimeLocal, meanDeltaTLocal, varDeltaTLocal,
471     meanDeltaTimpOverLocal, varDeltaTimpOverLocal, errorDeltaTimpLocal] =
472     bearingSignalModelLocal(d, D, contactAngle, n, faultType, fr, fc, fd, fm, N,
473     varianceFactor, fs, k, zita, fn, Lsdof, SNR_dB, qAmpMod);
474
475 %% Distributed fault
476 fs = 20000; % sample frequency [Hz]
477 SNR_dB = 0;
478 qFault = 1;
479 qStiffness = 0.1;
480 qRotation = 0.1;
481 [tDist, xDist, xNoiseDist, frTimeDist] = bearingSignalModelDist(d, D,
482     contactAngle, n, faultType, fc, fd, fm, fr, N, fs, SNR_dB, qFault, qStiffness,
483     qRotation);
484
485 function [t, x, xNoise, frTime, meanDeltaT, varDeltaT, meanDeltaTimpOver,
486     varDeltaTimpOver, errorDeltaTimp] = bearingSignalModelLocal(d, D,
487     contactAngle, n, faultType, fr, fc, fd, fm, N, varianceFactor, fs, k, zita, fn, Lsdof,
488     SNR_dB, qAmpMod)

```

```

488     %% Generation of a simulated signal for localized fault in rolling
489         element bearing
490
491     %
492     % Input:
493     % d = bearing roller diameter [mm]
494     % D = pitch circle diameter [mm]
495     % contactAngle = contact angle [rad]
496     % n = number of rolling elements
497     % faultType = fault type selection: inner, outer, ball [string]
498     % fr = row vector containing the rotation frequency profile
499     % fc = row vector containing the carrier component of the speed
500     % fm = row vector containing the modulation frequency
501     % fd = row vector containing the frequency deviation
502     % N = number of points per revolution
503     % varianceFactor = variance for the generation of the random
504         contribution (ex. 0.04)
505     % fs = sample frequency of the time vector
506     % k = SDOF spring stiffness [N/m]
507     % zita = SDOF damping coefficient
508     % fn = SDOF natural frequency [Hz]
509     % Lsdof = length of the in number of points of the SDOF response
510     % SNR_dB = signal to noise ratio [dB]
511     % qAmpMod = amplitude modulation due to the load (ex. 0.3)
512
513     %
514     % Output:
515     % t = time signal [s]
516     % x = simulated bearing signal without noise
517     % xNoise = simulated bearing signal with noise
518     % frTime = speed profile in the time domain [Hz]
519     % meanDeltaT = theoretical mean of the inter-arrival times
520     % varDeltaT = theoretical variance of the inter-arrival times
521     % menDeltaTimpOver = real mean of the inter-arrival times
522     % varDeltaTimpOver = real variance of the inter-arrival times
523     % errorDeltaTimp = generated error in the inter-arrival times
524
525     %
526     % G. D'Elia and M. Cocconcelli
527
528     if nargin < 14,

```

```

536         qAmpMod = 1;
537     end
538
539     switch faultType
540     case 'inner'
541         geometryParameter = 1 / 2 * (1 + d/D*cos(contactAngle)); % inner
542         race fault
543     case 'outer'
544         geometryParameter = 1 / 2 * (1 - d/D*cos(contactAngle)); % outer
545         race fault
546     case 'ball'
547         geometryParameter = 1 / (2*n) * (1 - (d/D*cos(contactAngle))^2)
548         /(d/D); % outer race fault
549     end
550
551     Ltheta = length(fr);
552     theta = (0:Ltheta-1)*2*pi/N;
553
554     deltaThetaFault = 2*pi/(n*geometryParameter);
555     numberOfImpulses = floor(theta(end)/deltaThetaFault);
556     meanDeltaTheta = deltaThetaFault;
557     varDeltaTheta = (varianceFactor*meanDeltaTheta)^2;
558     deltaThetaFault = sqrt(varDeltaTheta)*randn([1 numberOfImpulses-1]) +
559         meanDeltaTheta;
560     thetaFault = [0 cumsum(deltaThetaFault)];
561     frThetaFault = interp1(theta,fr,thetaFault,'spline');
562     deltaTimp = deltaThetaFault ./ (2*pi*frThetaFault(2:end));
563     tTimp = [0 cumsum(deltaTimp)];
564
565     L = floor(tTimp(end)*fs); % signal length
566     t = (0:L-1)/fs;
567     frTime = interp1(tTimp,frThetaFault,t,'spline');
568
569     deltaTimpIndex = round(deltaTimp*fs);
570     errorDeltaTimp = deltaTimpIndex/fs - deltaTimp;
571
572     indexImpulses = [1 cumsum(deltaTimpIndex)];
573     index = length(indexImpulses);

```

```

562 while indexImpulses(index)/fs > t(end)
563     index = index - 1;
564 end
565 indexImpulses = indexImpulses(1:index);
566
567 meanDeltaT = mean(deltaTimp);
568 varDeltaT = var(deltaTimp);
569 meanDeltaTimpOver = mean(deltaTimpIndex/fs);
570 varDeltaTimpOver = var(deltaTimpIndex/fs);
571
572 x = zeros(1,L);
573 x(indexImpulses) = 1;
574
575 % amplitude modulation
576 if strcmp(faultType, 'inner')
577
578     if length(fc) > 1,
579         thetaTime = zeros(1,length(fr));
580         for index = 2:length(fr),
581             thetaTime(index) = thetaTime(index - 1) + (2*pi/N)/(2*pi*
582                 fr(index));
583         end
584         fcTime = interp1(thetaTime,fc,t,'spline');
585         fdTime = interp1(thetaTime,fd,t,'spline');
586         fmTime = interp1(thetaTime,fm,t,'spline');
587
588         q = 1 + qAmpMod * cos(2*pi*fcTime.*t + 2*pi*fdTime.*(cumsum(cos
589             (2*pi*fmTime.*t)/fs)));
590     else
591         q = 1 + qAmpMod * cos(2*pi*fc*t + 2*pi*fd*(cumsum(cos(2*pi*fm*t)
592             /fs)));
593     end
594     x = q .* x;
595 end
596
597 [sdofRespTime] = sdofResponse(fs,k,zita,fn,Lsdof);
598 x = fftfilt(sdofRespTime,x);
599
600

```

```

607     L = length(x);
608     rng('default'); %set the random generator seed to default (for
609         comparison only)
610     SNR = 10^(SNR_dB/10); %SNR to linear scale
611     Esym=sum(abs(x).^2)/(L); %Calculate actual symbol energy
612     NO = Esym/SNR; %Find the noise spectral density
613     noiseSigma = sqrt(NO); %Standard deviation for AWGN Noise when x is real
614     nt = noiseSigma*randn(1,L);%computed noise
615     xNoise = x + nt; %received signal

616 function [t,x,xNoise,frTime] = bearingSignalModelDist(d,D,contactAngle,n,
617     faultType,fc,fd,fm,fr,N,fs,SNR_dB,qFault,qStiffness,qRotation)
618     %% Generation of a simulated signal for distributed fault in rolling
619     element bearing
620
621     %
622     % Input:
623     % d = bearing roller diameter [mm]
624     % D = pitch circle diameter [mm]
625     % contactAngle = contact angle [rad]
626     % n = number of rolling elements
627     % faultType = fault type selection: inner, outer, ball [string]
628     % fr = row vector containing the rotation frequency profile
629     % fc = row vector containing the carrier component of the speed
630     % fm = row vector containing the modulation frequency
631     % fd = row vector containing the frequency deviation
632     % N = number of points per revolution
633     % SNR_dB = signal to noise ratio [dB]
634     % qFault = amplitude modulation at the fault frequency
635     % qStiffness = amplitude value of the deterministic component related to
636         the stiffness variation
637     % qRotation = amplitude value of the deterministic component related to
638         the bearing rotation
639
640     %
641     % Output:
642     % t = time signal [s]
643     % x = simulated bearing signal without noise
644     % xNoise = simulated bearing signal with noise
645     % frTime = speed profile in the time domain [Hz]
646     %

```



```

620 % G. D'Elia and M. Cocconcelli
621
622 switch faultType
623     case 'inner'
624         geometryParameter = 1 / 2 * (1 + d/D*cos(contactAngle)); % inner
625         race fault
626     case 'outer'
627         geometryParameter = 1 / 2 * (1 - d/D*cos(contactAngle)); % outer
628         race fault
629     case 'ball'
630         geometryParameter = 1 / (2*n) * (1 - (d/D*cos(contactAngle))^2)
631         /(d/D); % outer race fault
632     end
633
634 Ltheta = length(fr);
635 theta = (0:Ltheta-1)*2*pi/N;
636 thetaTime = zeros(1,length(fr));
637 for index = 2:length(fr),
638     thetaTime(index) = thetaTime(index - 1) + (2*pi/N)/(2*pi*fr(index));
639 end
640
641 L = floor(thetaTime(end)*fs); % signal length
642 t = (0:L-1)/fs;
643 frTime = interp1(thetaTime,fr,t,'spline');
644
645 % generating rotation frequency component
646 xRotation = qRotation * cos(fc/fc.*theta + fd./fc.*(cumsum(cos(fm./fc.*
647     theta)/N)));
648 xRotationTime = interp1(thetaTime,xRotation,t,'spline');
649
650 % generating stiffness variation
651 tauStiffness = n / 2 * (1 - d/D*cos(contactAngle));
652 xStiffness = qStiffness * cos(fc./fc*tauStiffness.*theta + fd./fc*
653     tauStiffness.*(cumsum(cos(fm./fc*tauStiffness.*theta)/N)));
654 xStiffnessTime = interp1(thetaTime,xStiffness,t,'spline');
655
656 % amplitude modulation
657 tauFautl = n*geometryParameter;

```

```

658 q = 1 + qFault * sin(fc./fc*tauFault.*theta + fd./fc*geometryParameter
659     .*(cumsum(cos(fm./fc*geometryParameter.*theta)/N)));
660 qTime = interp1(thetaTime,q,t,'spline');
661 xFaultTime = randn(1,L);
662 xFaultTime = xFaultTime .* qTime;
663
664 % adding therms
665 x = xFaultTime + xStiffnesTime + xRotationTime;
666
667 % Adding noise with given SNR
668 rng('default'); %set the random generator seed to default (for
669     comparison only)
670 SNR = 10^(SNR_dB/10); %SNR to linear scale
671 Esym=sum(abs(x).^2)/(L); %Calculate actual symbol energy
672 NO = Esym/SNR; %Find the noise spectral density
673 noiseSigma = sqrt(NO); %Standard deviation for AWGN Noise when x is real
674 nt = noiseSigma*randn(1,L);%computed noise
675 xNoise = x + nt; %received signal

```

```

696 function [sdofRespTime] = sdofResponse(fs,k,zita,fn,Lsdof)
697     %% Acceleration of a SDOF system
698     [sdofRespTime] = sdofResponse(fs,k,zita,fn,Lsdof)
699     %
700     % Input:
701     % fs = sample frequency [Hz]
702     % k = spring stiffness [N/m]
703     % zita = damping coefficient
704     % fn = Natural frequency [Hz]
705     % Lsdof = desired signal length [points]
706     %
707     % Output:
708     % sdofRespTime = acceleration (row vector)
709     %
710     % G. D'Elia and M. Cocconcelli
711
712     m = k/(2*pi*fn)^2;
713     F = 1;
714     A = F/m;
715     omegan = 2*pi*fn;

```

```
720 omegad = omegan*sqrt(1-zita^2);
721
722
723 t = (0:Lsdof-1)/fs;
724 % system responce
725 xt = A/omegad * exp(-zita*omegan*t).*sin(omegad*t); % displacement
726 xd = [0 diff(xt)*fs]; % velocity
727 sdofRespTime = [0 diff(xd)*fs]; % acceleration
```